A model for membranes, vesicles and micelles in amphiphilic systems

1995 J. Phys.: Condens. Matter 7 5753

(http://iopscience.iop.org/0953-8984/7/29/005)

J. Phys.: Condens. Matter 7 (1995) 5753–5776. Printed in the UK

A model for membranes, vesicles and micelles in amphiphilic systems

A M Somoza†, E Chacón†‡, L Mederos† and P Tarazona§

† Instituto de Ciencia de Materiales, Consejo Superior de Investigaciones Científicas, E-28049 Madrid, Spain

‡ Departamento de Física Fundamental, Universidad Nacional de Educación a Distancia, Apartado 60141, E-28028 Madrid

§ Departamento de Física de la Materia Condensada, Universidad Autónoma de Madrid, E-28049 Madrid, Spain

Received 19 April 1995

Abstract. We present a microscopic model for the aggregates of amphiphilic molecules, based on a simple density functional approximation for the free energy. The different molecular aggregates are described as self-structured density distributions at the relative minima of the grand potential energy. We search for these structures with planar and spherical geometries, and obtain the phase diagram for bilayer membranes, and the curvature energies for vesicles and different types of micelles. The study of a global phase diagram, to get the density of micelles and isolated amphiphilic molecules, at equilibrium with free membranes, requires the link between two description levels of micelles: as self-structured density distributions, or as molecular clusters in the solution of amphiphilic molecules in water. This is done with the help of a simple harmonic model which provides an appropriate choice of the configurational unit cell for micelles.

1. Introduction

Amphiphilic molecules are complex, flexible structures with a polar group in the 'head' and one or several hydrocarbon 'tails'. The polar head is hydrophilic—it would be easily dissolved in water—while the hydrocarbon tails are hydrophobic and they would segregate like oil in water. The presence of both trends in the same molecule implies the frustration of these opposite tendencies, and the result is the large variety of aggregation structures which are observed in these systems: micelles, membranes, bicontinuous foams, inverse micelles, etc; with aggregation scales going from the molecular size, to mesoscopic structures and up to macroscopic phases [1–3]. The smallest aggregates are spherical micelles, which are clusters up to few hundred molecules, with the polar heads in the surface with water and the hydrocarbon tails in the interior. A solution of water with micelles may be regarded as an extreme case of non-ideal solution with strong clustering effects. Rod-like micelles and membranes are clusters which become mesoscopic in one or two dimensions. In particular, membranes are two-dimensional structures with molecular width in the other direction. The extensive properties in a membrane are proportional to the surface area, so we may describe it as a dense two-dimensional phase in thermodynamic coexistence with the dilute water solution. At higher concentration of amphiphilic molecules in water, the micelles or membranes interact with each other and produce other three-dimensional phases, like micelle crystals, lamellar phases and more complex structures. The most relevant characteristic of

0953-8984/95/295753+24$19.50

these phases is that they combine different levels of organization, at very different scales and without a rigid hierarchy between them [1–3].

The theoretical understanding of these systems poses a tremendous challenge [4]. The complexity of the molecules and their interactions renders impossible any first-principles description at microscopic level. The description through effective models has been successfully attempted for several aspects. Thus, the micelles may be described as droplets of hydrocarbon liquid with the polar heads anchored at the surface with water, limiting the droplet size [5, 6]. On the other hand, free membranes may be described by effective surface hamiltonians, which treat them as geometrical surfaces with empirical thermodynamic parameters [7–10]. Studies within this formalism have produced interesting advances in the understanding of the geometrical shapes of closed membranes (vesicles) and of the entropy associated with the fluctuation of the membrane. However, these approaches cannot be used to address questions which involve both microscopic and mesoscopic structures. The phase diagram for free membranes in a solution would require a consistent treatment of micelles and membranes at microscopic level, to get the total amount of amphiphilic molecules dissolved in water (either as micelles or as isolated molecules) when the membranes are at thermodynamic equilibrium. The same applies to many other problems in the physics of biomembranes [11], like the fusion of two membranes to form a single surface, the segregation of vesicles or the preferential nucleation on a substrate. Moreover, the empirical parameters used in the effective surface hamiltonians should be related at molecular level, e.g. the curvature and edge energies are not independent parameters and this may condition the threshold for the transformation of open membranes in closed vesicles [9, 10]. All these questions require a treatable microscopic model, which, keeping the essential features of the molecular interactions, may be used to study mesoscopic and microscopic aggregates. The model presented here goes beyond simplified lattice-gas representations [12–14] and Ginzburg–Landau theories [15], which are useful stepping stones but have strong restrictions in the possible types of aggregates and in the relation with molecular models.

The idea is to use the density functional formalism [16] for the free energy, $F[\rho]$, and to describe the aggregates as local minima of the grand potential energy, $\Omega = F - \mu N$, at given temperature, T, and chemical potential μ. In section 2 we present the simple density functional approximation used here and the method used to search for local minima of the grand potential energy. In sections 3 and 4 we study relative minima with planar and spherical geometries respectively, to describe flat membranes, vesicles and micelles of different types. In this approach, we may take advantage of the experience in the description of structured phases, like crystals [17, 18] and liquid crystals [19, 20], but we should point out an important difference which emerges in the study of the global phase diagram in section 5. In any description of self-structured systems as inhomogeneous density distributions, we have to pin down the inhomogeneity to an arbitrary origin and orientation. The degrees of freedom associated to this choice should be taken into account in the total entropy. In a three-dimensional phase, like a crystal, there are only a few degrees of freedom associated with the position and orientation of the whole macroscopic system, and we may neglect them in the thermodynamic limit. However, if we describe micelles as bulges in the density distribution, the degrees of freedom associated with their position in space give an important contribution to the total entropy and they have to be included to obtain the global phase diagram, i.e. to calculate the density of micelles in the solution of amphiphilic molecules in water. But there is not a well defined separation between those degrees of freedom which have to be added and those already included in any approximate density functional, used to characterize the structure of the droplets as local minima of the grand potential energy. We find in the literature different ways of tinkering with this problem. Some authors regard

the inhomogeneous density distribution as a description from the centre of mass of the aggregate, and add the translational degrees of freedom as those of a particle with the total mass of the aggregate [6]. The trouble with that approach is that the prediction for the density of micelles in a solution of amphiphilic molecules depends on the mass of the amphiphilic molecules, through the 'thermal wavelength' of the micelles, while in classical statistical mechanics all the equilibrium properties associated to spatial distributions have to be independent of the particle masses. In other cases, the problem is hidden with the use of dimensionless densities, in terms of any natural parameter of the model [21]. In the context of nucleation theory, the separation between the two levels of description is rationalized by regarding the inhomogeneous density distributions as the local minima of a 'coarse grained' density functional. In the absence of any external symmetry-breaking potential the coarse grained free energy is degenerated with respect to the position of the droplets and the associated 'Goldstone modes' may be integrated to get the remaining entropy [22], but we still lack of a well defined correspondence between the approximate density functionals and the coarse-graining length scale. The relative success of the theories following these different approaches is shown in the fact that, for well characterized molecular aggregates like droplets or amphiphilic micelles with a few hundred molecules, there is a large range of scales over which we may drop the uncertainty without qualitative changes. We have analysed the problem in a very simple model, presented in the appendix, for which we may compare the exact solution with approximate descriptions along the lines presented here. The comparison clarifies the problem and suggests a possible solution which is used in section 5 to get the global phase diagram of the system, linking the description of the molecular structure of the micelles with the density of these micelles in the solution.

In the case of membranes the problem is weaker, because they extend over mesoscopic distances in two dimensions, and it has been analysed more carefully [23]. The few degrees of freedom associated to the global translation and orientation are irrelevant because we treat the membranes as 'macroscopic' objects with extensive thermodynamic properties. The trouble comes from their character of two-dimensional objects in a three-dimensional space. In the absence of external potentials or restrictions, a large free membrane will always be deformed, because the deformation energy goes to zero in the long-wavelength limit of the corrugation. The correlation in the orientation of different pieces in a membrane decays beyond a given distance, called the persistence length, ξ. The membrane gains entropy with the corrugation, which is not included in the description as a fixed density distribution, either flat or with any other fixed shape. Theoretical analysis with surface hamiltonians give this length, ξ, from the ratio between the curvature energy and k_BT. If the membrane linear size is much shorter than the persistence length we may consider it as essentially flat (or spherical), but in strong amphiphiles, the size is still large enough to treat them as macroscopic objects. Nevertheless, our results may also be used to provide the empirical parameters in a surface hamiltonian, which include the effects of corrugation with different techniques.

2. Free energy density functional model

Our objective here is to develop a minimal model for a system of amphiphilic molecules in water. The description of these molecules has to include the presence of opposite tendencies in each molecular side, but we neglect the role of flexible chains or other internal degrees of freedom. We describe the amphiphilic as rigid anisotropic molecules with one preferential axis, its direction being given by a unit vector $\hat{\boldsymbol{u}}$. The distribution function of amphiphilic molecules, $\rho(\boldsymbol{r}, \hat{\boldsymbol{u}})$, gives the average density of molecules with orientation $\hat{\boldsymbol{u}}$ and position $\boldsymbol{r}$.

The interaction of the amphiphile with water is the driving force for the formation of complex aggregates, but we may simplify the description by considering only the distribution of the amphiphile and the effective interaction between them which results from the solvation forces induced by the water. We describe this effective interaction through a potential energy $\Phi(\boldsymbol{r}_1 - \boldsymbol{r}_2, \hat{\boldsymbol{u}}_1, \hat{\boldsymbol{u}}_2)$, which depends on the relative position and on the orientation of two amphiphilic molecules. As is usually done in molecular fluids [24], we may expand this potential in terms of independent rotational invariants, like the relative distance between the molecular centres, $r_{12} = |\boldsymbol{r}_1 - \boldsymbol{r}_2|$, the projection of the molecular axis on the direction of the relative position, $\hat{\boldsymbol{u}}_1 \cdot \hat{\boldsymbol{r}}_{21}$ and $\hat{\boldsymbol{u}}_2 \cdot \hat{\boldsymbol{r}}_{21}$ (with $\hat{\boldsymbol{r}}_{21} = (\boldsymbol{r}_2 - \boldsymbol{r}_1)/r_{12}$), and the angle $\phi_2 - \phi_1$ between the projections of $\hat{\boldsymbol{u}}_1$ and $\hat{\boldsymbol{u}}_2$ in the plane perpendicular to $\hat{\boldsymbol{r}}_{21}$. For a general pair interaction between molecules with axial symmetry, we have:

$$\Phi(\boldsymbol{r}_1 - \boldsymbol{r}_2, \hat{\boldsymbol{u}}_1, \hat{\boldsymbol{u}}_2) = \sum_{l_1, l_2 = 0}^{\infty} \sum_{m} \xi^m_{l_1, l_2}(r_{12}) P^m_{l_1}(\hat{\boldsymbol{u}}_1 \cdot \hat{\boldsymbol{r}}_{21}) P^{-m}_{l_2}(-\hat{\boldsymbol{u}}_2 \cdot \hat{\boldsymbol{r}}_{21})\, \mathrm{e}^{\mathrm{i}(\phi_2 - \phi_1)\, m} \tag{1}$$

where $P^m_i(x)$ are the associated Legendre functions and the index m runs for $|m| \leqslant \min(l_1, l_2)$.

The first term in the series is the isotropic potential energy $\xi^0_{00}(r)$, given by the full angular average of the interactions. In our case this should be essentially repulsive, because an attractive contribution would produce a segregation in water-rich and amphiphilic-rich bulk fluid phases, which should not appear. As the simplest choice of a repulsive isotropic interaction we take it to be the hard-sphere (HS) potential, $\Phi_{HS}(r)$, with a sphere diameter which we take as the unit length.

The next twin terms in (1),with $\xi^0_{10}(r) = \xi^0_{01}(r) \equiv \Phi_1(r)$, include the polar interaction of one molecule independently of the orientation of the second molecule. These terms are the basic driving force to the formation of micelles and membranes: the attraction of the polar head in the amphiphilic molecule towards the water molecules. In our effective description this is represented by a repulsion from other amphiphilic molecules, irrespective of their orientation, because their presence implies the absence of water. As a minimal model we may truncate the series (1) at this level to get

$$\Phi(\boldsymbol{r}_1 - \boldsymbol{r}_2, \hat{\boldsymbol{u}}_1, \hat{\boldsymbol{u}}_2) = \Phi_{HS}(r_{12}) + \Phi_1(r_{12}) \left[(\hat{\boldsymbol{u}}_1 \cdot \hat{\boldsymbol{r}}_{21}) - (\hat{\boldsymbol{u}}_2 \cdot \hat{\boldsymbol{r}}_{21}) \right]. \tag{2}$$

A similar potential has been proposed by Telo da Gama [25] to study ternary mixtures of amphiphilic surfactant in water–oil systems, with polar interaction of the surfactant with the molecules of oil and water, plus isotropic, Lennard-Jones like, interactions among all the components to get the water–oil segregation. Here we begin with a binary system of water and amphiphile, and simplify it further to keep only the amphiphilic molecules. The effective polar interaction between them would arise from the direct water–amphiphile polar interaction in that model, through the molecular correlations. The simplification in our model allows us to include a better approximation for the free energy as a function of $\rho(\boldsymbol{r}, \hat{\boldsymbol{u}})$ and to search for different types of molecular aggregates. Instead of a simple local density approximation for the hard-sphere repulsion, we include a non-local density functional [26] which has proved to be very reliable for the description of packing effects, including the layering and the crystallization of the fluid at high density. This is of little importance in smooth fluid interfaces but in our case the packing effects have to appear in the size and structure of micelles and in the bilayer structure of membranes. The soft anisotropic interactions Φ_1 may be included in a mean field approximation, which has proved to be qualitatively correct in the description of interfaces and other inhomogeneous systems [16].

The molecular distribution function is factorized as $\rho(\boldsymbol{r}, \hat{\boldsymbol{u}}) = \rho(\boldsymbol{r})\alpha(\boldsymbol{r}, \hat{\boldsymbol{u}})$, with the density distribution $\rho(\boldsymbol{r})$ and the normalized distribution of molecular orientations $\alpha(\boldsymbol{r}, \hat{\boldsymbol{u}})$. The approximation for the free energy functional is

$$F[\rho(\boldsymbol{r}, \hat{\boldsymbol{u}})] = F_{HS}[\rho(\boldsymbol{r})] + k_B T \int \mathrm{d}\boldsymbol{r}_1 \int \mathrm{d}\hat{\boldsymbol{u}}_1 \; \rho(\boldsymbol{r}_1)\alpha(\boldsymbol{r}_1, \hat{\boldsymbol{u}}_1) \log(4\pi\alpha(\boldsymbol{r}_1, \hat{\boldsymbol{u}}_1)) + \int \mathrm{d}\boldsymbol{r}_1 \int \mathrm{d}\hat{\boldsymbol{u}}_1 \int \mathrm{d}\boldsymbol{r}_2 \; \rho(\boldsymbol{r}_1)\alpha(\boldsymbol{r}_1, \hat{\boldsymbol{u}}_1)\rho(\boldsymbol{r}_2)\Phi_1(r_{12})(\hat{\boldsymbol{r}}_{21} \cdot \hat{\boldsymbol{u}}_1) \tag{3}$$

where we have separated the contribution of the isotropic hard-sphere fluid, the ideal gas contribution of the molecular orientations and the mean field contribution of the anisotropic interaction.

The HS free energy depends only on the density distribution $\rho(\boldsymbol{r})$, it includes the translational contribution from the ideal gas free energy and the free energy excess due to the packing restrictions. The later is approximated [26] by the free energy excess per molecule, $\psi_{HS}(\rho)$, at an 'average density', $\bar{\rho}(\boldsymbol{r})$:

$$F_{HS}[\rho(\boldsymbol{r})] = k_B T \int \mathrm{d}\boldsymbol{r}_1 \; \rho(\boldsymbol{r}_1)\,(\log(\rho(\boldsymbol{r}_1)) - 1) \; + k_B T \int \mathrm{d}\boldsymbol{r}_1 \; \rho(\boldsymbol{r}_1)\psi_{HS}(\bar{\rho}(\boldsymbol{r}_1)). \tag{4}$$

The truncation of the interaction potential (1) at the level of (2) pays off now by an important simplification of the problem. For a given temperature and chemical potential we have to search for local minima of the grand potential energy

$$\Omega = F - \mu N \tag{5}$$

with respect to the distribution function $\rho(\boldsymbol{r}, \hat{\boldsymbol{u}})$, but the minimization with respect to the distribution of molecular orientations $\alpha(\boldsymbol{r}, \hat{\boldsymbol{u}})$ may be done analytically:

$$\frac{\delta F[\rho(\boldsymbol{r}, \hat{\boldsymbol{u}})]}{\delta\alpha(\boldsymbol{r}_1, \hat{\boldsymbol{u}}_1)} = k_B T\rho(\boldsymbol{r}_1)\log(\alpha(\boldsymbol{r}_1, \hat{\boldsymbol{u}}_1)) + \int \mathrm{d}\boldsymbol{r}_2 \; \rho(\boldsymbol{r}_2)\Phi_{101}(r_{12})(\hat{\boldsymbol{r}}_{21} \cdot \hat{\boldsymbol{u}}_1) = Q(\boldsymbol{r}_1) \tag{6}$$

where $Q(\boldsymbol{r}_1)$ is a Lagrange multiplier to achieve the normalization of $\alpha(\boldsymbol{r}_1, \hat{\boldsymbol{u}}_1)$ integrated over molecular orientations. This leads to

$$\alpha(\boldsymbol{r}_1, \hat{\boldsymbol{u}}_1) = \exp[\boldsymbol{a}(\boldsymbol{r}_1) \cdot \hat{\boldsymbol{u}}_1] \Big/ \int \mathrm{d}\hat{\boldsymbol{u}}_2 \; \exp(\boldsymbol{a}(\boldsymbol{r}_1) \cdot \hat{\boldsymbol{u}}_2) \tag{7}$$

where the vector field $\boldsymbol{a}(\boldsymbol{r}_1)$ is defined as

$$\boldsymbol{a}(\boldsymbol{r}_1) = \frac{1}{k_B T} \int \mathrm{d}\boldsymbol{r}_2 \; \rho(\boldsymbol{r}_2)\Phi_1(|\boldsymbol{r}_1 - \boldsymbol{r}_2|)\frac{(\boldsymbol{r}_1 - \boldsymbol{r}_2)}{|\boldsymbol{r}_1 - \boldsymbol{r}_2|}. \tag{8}$$

By substitution of (7–8) into (3) we get a free energy density functional, which is already minimized with respect to the molecular orientations:

$$F[\rho(\boldsymbol{r})] = \mathrm{Min}\{F[\rho(\boldsymbol{r}, \hat{\boldsymbol{u}})]\}_\alpha = F_{HS}[\rho(\boldsymbol{r})] \; - \; k_B T \int \mathrm{d}\boldsymbol{r} \; \rho(\boldsymbol{r}) \log\left(\frac{\sinh(|\boldsymbol{a}(\boldsymbol{r})|)}{|\boldsymbol{a}(\boldsymbol{r})|}\right) \tag{9}$$

where the effects of the anisotropic interactions are described through the auxiliary field (8). Notice that although we started in (3) with a mean field description of the anisotropic pair interactions, hence proportional to $\rho(\boldsymbol{r}_1)\rho(\boldsymbol{r}_2)$, the average over the molecular orientations induces in (9) higher-order terms in the density distribution, which may be interpreted as effective many-molecule interactions. These terms stabilize finite molecular aggregates, which do not grow into macroscopic bulk phases. The same type of effective free energy has been used in lattice models [12, 13, 14]. In the absence of external potentials, this

density functional always has a stationary grand potential energy for a homogeneous density distribution $\rho(r) = \rho_0$, which gives $a = 0$ in (8), and it represents a phase of surfactant molecules with random orientations, which in our model becomes equivalent to a HS fluid. The density of this homogeneous solution is used to control the chemical potential, $\mu_0 = \mu_{HS}(\rho_0)$, in our search for inhomogeneous density distributions.

For low values of μ (and ρ_0) the homogeneous phase represents a dilute solution of amphiphilic molecules in water and we may find other local minima of the grand potential energy,

$$\Omega[\rho(r)] = F[\rho(r)] - \mu_{HS}(\rho_0) \int dr\ \rho(r) \tag{10}$$

for non-uniform density distributions, which represent the different types of molecular aggregates. In the next two sections we search for those minima with two different geometries, planar and spherical. In each case, the minimization of (10) is done by conjugate gradient techniques, from a judicious initial guess for the density distribution, or through a variational minimization within a functional family. The structures obtained and the thermodynamic interpretations are different for each case, but they result from the same microscopic model (3), and we may relate the properties of very different types of aggregates by making reference to their common thermodynamic parameters. In this work we always stay in the limit of dilute amphiphilic solutions, $\rho_0 \leqslant 0.05$ in units of the HS diameter, and the aggregates to be found will form ideal solutions of micelles, free membranes or vesicles, but without important interactions between the aggregates. The case of dense amphiphilic phases is left for future work.

It remains to specify the function $\Phi_1(r)$ which in our model mimics the complex molecular interactions of real amphiphilic molecules. We have studied several functional forms, the simplest one is an empty core Yukawa potential,

$$\Phi_1(r) = \begin{cases} (C/r)e^{-\lambda(r-1)} & \text{for } r \geqslant 1 \\ 0 & \text{for } r < 1 \end{cases} \tag{11}$$

with r in units of the HS diameter. The coefficient C represents the maximum absolute value of the anisotropic interaction energy between two amphiphilic molecules, and we take it as our unit of energy and temperature. In accordance with (2) the function $\Phi_1(r)$ is positive if the vector $\hat{u}$ is defined as pointing from the hydrocarbon tail towards the polar head of the molecule. The parameter λ measures the relative range of the polar interaction with respect to the isotropic hard core and we present results with several values of this parameter. We have also explored the behaviour of the system for other functional forms, like a double Yukawa and Lennard-Jones type of interactions, to separate the maximum of $\Phi_1(r)$ from the hard core $r = 1$, and some results are commented below.

3. Planar membranes

We search for non-trivial relative minima of (10) with a density profile, $\rho(z)$ which depends only on one cartesian coordinate z. The vector field $a(r)$ is parallel to the axis director $\hat{z}$, and the distribution of molecular orientations will depend only on z and $\hat{u} \cdot \hat{z}$. The molecular orientation order parameter,

$$\eta(z) = \int d\hat{u}\ \alpha(z, \hat{u})\ \hat{u} \cdot \hat{z} \tag{12}$$

measures the degree of 'polar' order with respect to the z axis. Thus, $\eta = 1$ and -1 represent preferential orientations parallel and antiparallel to the direction given by a $\hat{z}$.

The density profile should go to the homogeneous density ρ_0 (and random orientations $\eta = 0$) for z far away from an arbitrary origin, to represent an isolated planar aggregate of amphiphilic molecules. The search is done by discretizing z in small steps (up to 100 per HS diameter) and minimizing the grand potential energy (10), with a conjugated gradient method from an initial density profile with a bump around the origin. From the density profile at the relative minimum we may use equations (7) and (8) to get the distribution of molecular orientations. Depending on the values of the temperature and chemical potential, the minimization may lead to the trivial homogeneous limit or to a structured profile, as shown in figure 1, with two parallel layers of molecules with opposite orientations, typical of the bilayer structure in amphiphilic membranes. Once we have found one of these structures we may also use it as an initial guess for different thermodynamic conditions. In any case we never found more than one type of stable structure for the same values of T and ρ_0, unless the initial guess contained several, well separated, density peaks which may generate different parallel membranes. At higher values of the bulk density ρ_0 the membranes may pack into a modulated dense phase. In the limit of low bulk density, the stable isolated membrane may be regarded as an 'interface' between two identical phases. The interfacial excess of grand potential energy per unit area, A,

$$\sigma(T, \rho_0) = \frac{\Omega[\rho(z)] - \Omega[\rho_0]}{A} \tag{13}$$

is the surface tension of the membrane. For $\sigma > 0$ the membrane is stable only if its total area A is kept constant by an external constraint, and the absolute minimum of the total grand potential energy corresponds to the absence of membrane. However, by increasing the bulk density or decreasing the temperature we may lower σ down to zero, along a line $\rho_0^{eq}(T)$ in the (T, ρ_0) plane. The coexistence line may also be calculated within a parametrized family of variational density profiles, which improves the computational efficiency (particularly at low ρ_0) without important changes in the results. We have used profiles parametrized as two gaussian peaks, with their width, separation and total integral used as variational parameters. In figure 2 we present the coexistence line for the Yukawa parametrization (11) for $\Phi_t(r)$, $\lambda = 3$, with the bulk density changing from $\rho_0 = 10^{-7}$ to 0.05 (in units of the HS diameter). At high density we compare the results of the conjugate gradient minimization with that of the gaussian parametrization, which is used at the lower values of ρ_0. Along this line a free membrane will be at equilibrium with the bulk dilute solution of amphiphilic molecules. The total grand potential energy will be independent of the area. Tresspassing across the equilibrium line the membranes would have negative excess of Ω, and they would grow without limits other than the total amount of molecules present in the system. In this respect we may consider the membrane as a phase at coexistence with the dilute solution, with the peculiarity that it is only extensive in two dimensions. If the total amount of amphiphilic molecules present in the system is large enough, the membrane would form with a total area A such that the remaining density in the bulk stays exactly at the coexistence line.

The structure of the membrane changes smoothly along the coexistence line, but always keeping the structure with two well defined molecular layers, and nearly saturated opposite polar orientational parameter $\eta \approx \pm 1$. There is a shallow depletion of molecules in the neighbourhood of the bilayer, but given the low bulk density it is hardly visible at the scale of the density peaks. The two peaks in the density profile of a bilayer become sharper at lower temperature and bulk density. The two-dimensional density of each layer in the the membrane, ρ_p, defined as half the excess of molecules per unit area, is controlled at low T and ρ_0 by the two-dimensional packing, it becomes independent of the value of λ (as shown in figure 3(a)) and it takes values close to or above the melting density for hard discs.

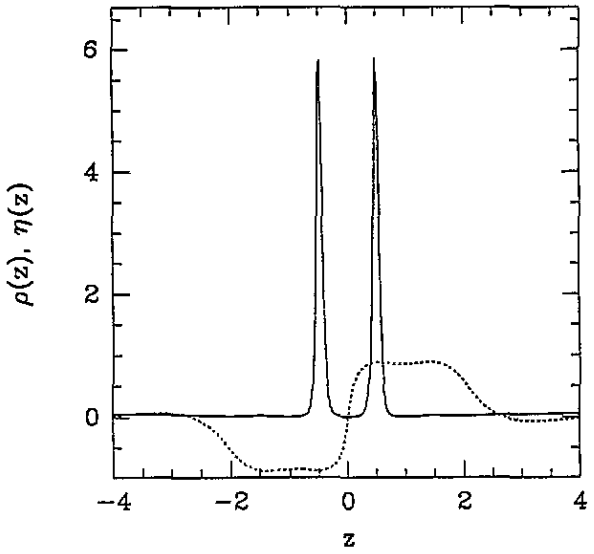

Figure 1. Density profile, $\rho(z)$ (full line) and polar order parameter, $\eta(z)$ (dotted line), for a bilayer membrane at equilibrium, $\sigma = 0$, with a bulk density $\rho_0 = 0.05$ and a Yukawa interaction with $\lambda = 3$. The two layers in the membrane have opposite orientations with $\eta \approx \pm 0.9$, the regions with strong order in the molecular orientation go well beyond the layers, over the regions where the bulk density is depleted below the bulk value. The HS diameter is used to provide the units of distance and density.

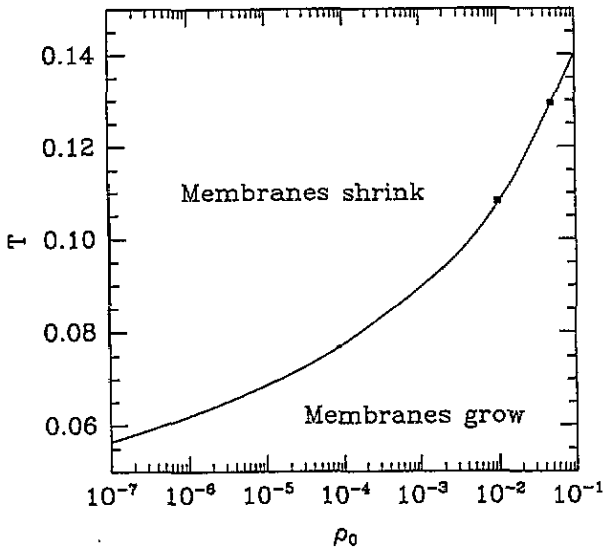

Figure 2. Equilibrium line for bilayer membranes with polar interaction range $\lambda = 3$, in the Yukawa potential. The temperature is in units of C/k_B, equation (11), and the bulk density ρ_0 is in units of the HS diameter. Along the line, $\rho_0^{eq}(T)$, we get membranes with zero surface tension, calculated through a variational minimization of Ω with a double gaussian parametrization of the density profile. The squares give the results with the full conjugated gradient minimization with respect to $\rho(z)$.

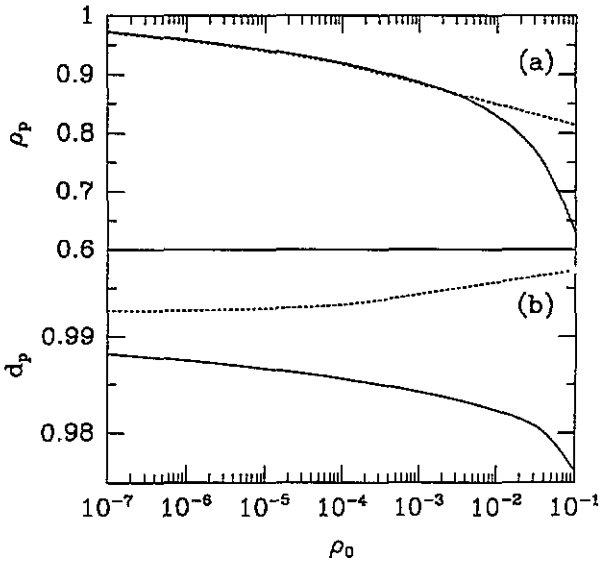

Figure 3. Parameters of the bilayer membranes along the coexistence lines for two values of the polar interaction range $\lambda = 2$ (dotted line) and 3 (full line) The horizontal axis gives the bulk density ρ_0, but it implies also a change in the temperature, to keep along the equilibrium line (figure 2). In (a) we present the two-dimensional density of each peak, ρ_p, in the density profile of the membrane, i.e. half the excess of molecules per unit area, in units of the HS diameter. In (b) we present the distance between the two peaks, d_p, which is always very close to the HS diameter, but with different trends for the two values of λ.

This means that along the coexistence line there should be a transition from liquid to solid membranes, which is not included in our variational minimization of the grand potential energy. As T and ρ_0 increase we observe, for $\lambda = 3$ in figure 3(a), a decrease of ρ_p in a regime where the density of the membrane depends on the range of the soft anisotropic interactions. The separation between the two layers in the membrane is always close to the contact distance of the HS cores in each layer (figure 3(b)), but the small variations along the coexistence line have different trends for $\lambda = 2$ and 3.

The structure of the membrane changes qualitatively if the parameter λ is small enough. For $\lambda < 1.5$ we observe the appearance of structures like 'tetra-layers' with four peaks in the density distribution, because the polar interaction is acting through distances of several times the molecular size. This is clearly unphysical, given our interpretation of the amphiphile–amphiphile interaction as an effective way to represent the presence or absence of water near each amphiphile molecule. Thus, we restrict ourselves to values of $\lambda \geqslant 1.5$. If the bulk density ρ_0 is increased we found that the homogeneous bulk becomes unstable and the system develops a layered structure, which may be regarded as a signature of a lamellar phase. A prelude of this phase is observed in the presence of a very weak effective attraction between two parallel membranes, induced by shallow depletion in the density profile in the neighbourhood of each bilayer. For the bulk densities considered here this attraction (proportional to ρ_0) is so small that it would be easily overtaken by other effects, like the entropic Helfrich interaction [27] which creates an effective repulsion between membranes.

We have found the same qualitative behaviours for membranes with a broad variety of functional forms for the interaction $\Phi_1(r)$ and the inclusion of some higher-order terms in

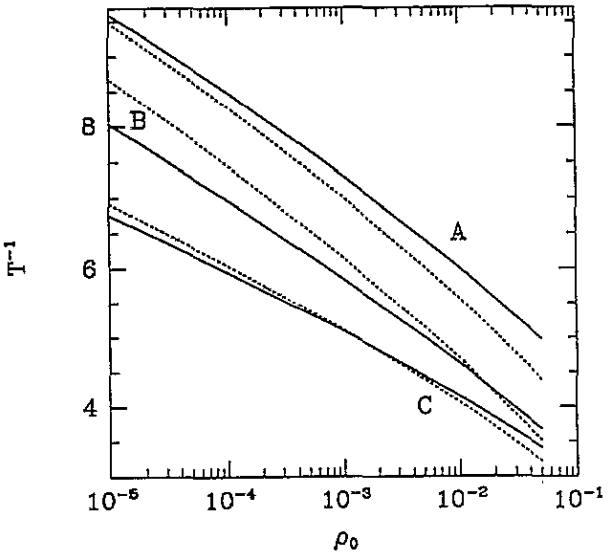

Figure 4. Equilibrium lines $\rho_0^{eq}(T)$ for bilayer membranes (full lines) and micellation lines $\rho_0^{mi}(T)$ (dotted lines) for several molecular interactions. The lines are represented in the $(\log(\rho_0), T^{-1})$ plane, in units of the HS diameter and the strength of the polar interaction C/k_B in the Yukawa potential (11). All the results include polar and quadrupolar interactions, equation (15), with the same Yukawa potential and with $\Phi_2(r) = q\Phi_1(r)$. In (A), (B) we present the results for $\lambda = 2$ and two values of the quadrupolar interaction $q = 0.3$ (A) and $q = 0.5$ (B), while (B,) (C) correspond to the same value of $q = 0.5$ and two different values of the interaction range, (B) $\lambda = 2.$ and (C) $\lambda = 1.5$, the curves (B) have been shifted one vertical unit down to avoid overlap.

(1). The coexistence line changes with the interaction potential but always keeps the same trends, which are not far from straight lines in the $(T^{-1}, \log(\rho_0))$ plane, as shown in figure 4. At this stage we could conclude that the detailed form of the interaction potential (11), seems to be of little relevance for the qualitative properties of the system. However, the results presented in the next section for vesicles and micelles show that the global behaviour of the system is much more sensitive to the details of the interactions.

4. Vesicles and micelles

We turn now to search relative minima of the grand potential energy (10) with spherical symmetry, $\rho(\mathbf{r}) = \rho(r)$. The vector field $a(\mathbf{r})$ is radial and the orientational distribution depends only on r and $\hat{\mathbf{r}} \cdot \hat{\mathbf{u}}$. We may define the 'spherical' version of the order parameter η defined in (12). The numerical method used to locate these minima is similar to that used in the planar case, although more cumbersome to implement. We have used both conjugated gradient minimization with the radial density distribution discretized over a mesh, and several variational parametrizations to explore more efficiently the effect of the different interaction potentials. Our motivation is twofold: the study of vesicles and micelles.

First we may expect to find relative minima for structures similar to the planar membranes but closed on a sphere of radius R, which is large compared with the molecular size. This would represent a vesicle; they are known to form spontaneously in these systems [9]. The grand potential energy of these vesicles should have an extensive term, σA, where $A = 4\pi R^2$ is the total area and σ is the surface tension of the planar membrane (13). The

effect of the curvature should be proportional to R^{-2} times the total area, which gives a constant independent of the radius R. In the language of effective surface hamiltonians [10] we have:

$$\Omega_v(R) = 4\pi R^2\sigma + 4\pi(2\kappa + \kappa_g) + \text{terms of order } R^{-2} \ldots \tag{14}$$

where κ and κ_g are the elastic constants associated to normal and gaussian curvatures respectively. The study of these vesicles within our density functional approximations would allow us to get the curvature energy and its variation along the coexistence line of free membranes. In the spherical case the two constants appear in the linear combination $\kappa_s = \kappa + \kappa_g/2$, to which we refer below. The independent determination of the two constants could also be made within our approach, by considering density distributions with cylindrical symmetry and/or periodic corrugations in a flat membrane.

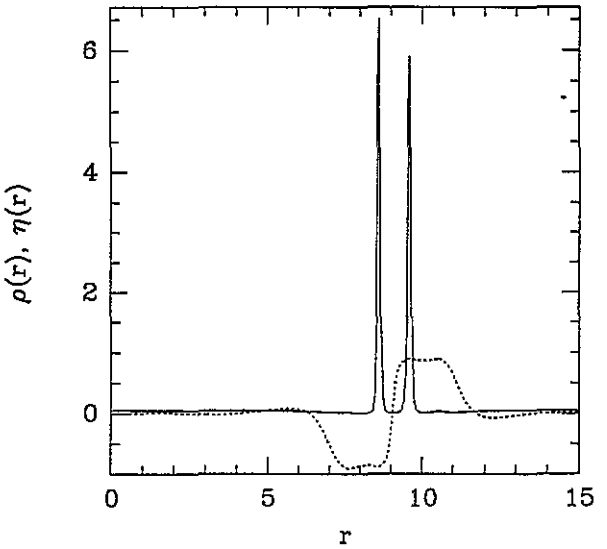

Figure 5. Radial density profile, $\rho(r)$, (full line) and polar order parameter, $\eta(r)$, (dotted line), for a spherical vesicle with a bulk density $\rho_0 = 0.05$ and for a polar interaction with a Yukawa range parameter $\lambda = 3$. The asymmetry between the inner and the outer layer, reflects the curvature effects in the profiles.

Starting with adequate initial guesses (e.g. the planar density profiles of section 3, centred around a radial distance $r = R$) it is easy to generate local minima of the grand potential energy, which have some asymmetry between the inner and the outer layer (figure 5) but still keep the same qualitative features of the planar membrane. Notice that in this geometry there is no restriction in the total area of the vesicle, the radius R may be defined somewhere in the middle of the bilayer structure, so that R, and hence the nominal area of the vesicle, may change with the functional variable $\rho(r)$. If we try to study a vesicle very far away from the line of coexistence for free membranes, the minimization of Ω with respect to the density profile would lead to growing (for $\sigma < 0$) or decreasing (for $\sigma > 0$) values of R, up to the limit of our numerical mesh or down to the molecular size. Only at the coexistence curve, $\sigma = 0$, should we expect to stabilize vesicles, with a total grand potential energy which becomes constant independent of the radius for large R. In practice, the discretization of $\rho(r)$ on a mesh induces some 'numerical roughness' in Ω and in the neighbourhood of the free membrane coexistence line we may obtain stationary vesicles

with the size controlled by the initial input. With the minimization of (10) restricted to a variational family it is simple to include R as a fixed parameter (e.g. defined as the central point between the two gaussian peaks) to obtain vesicles of any radius. In any case for values of R larger than six or eight HS diameters, the excess of grand potential energy follows rather well the linear behaviour with the area (14), as shown in figure 6. From the slope of these lines we may get the surface tension, in agreement with its independent calculation for planar membranes. The extrapolation of the lines to $R = 0$ gives the curvature energy $8\pi\kappa_s$, which at equilibrium ($\sigma = 0$) becomes independent of the arbitrary choice of the nominal radius or area of the vesicle.

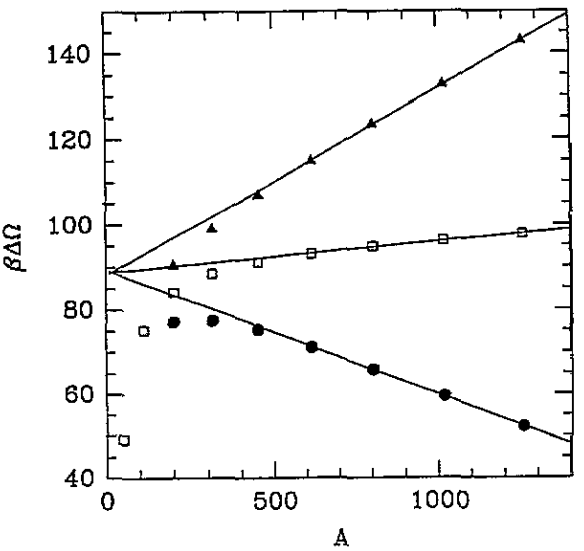

Figure 6. Excess of grand potential energy, $\beta\,\Delta\Omega = \Delta\Omega/k_BT$, for vesicles as a function of the total area, A, in units of the HS diameter. The data correspond to pure polar interaction with $\lambda = 2$ in the Yukawa interaction, equations. (2) and (11), with bulk density $\rho_0 = 0.02$, in units of the HS diameter, and three different temperatures very close to the equilibrium line for membranes: $k_BT/C = 0.1908$ (full triangles), 0.1913 (open squares) and 0.1918 (full circles). The straight lines are the linear fits to the data with the four largest values of the area. The slope is the surface tension of the membrane (which changes sign with the temperature) and the extrapolation to $A = 0$ gives the curvature energy $8\pi\kappa_s/(k_BT)$, which is very similar for the three temperatures. The actual value of $\Delta\Omega$ for vesicles of small area moves away from the straight line towards the grand potential excess of micelles.

Our first results were puzzling because we got negative curvature constants. This would imply not only the intrinsic instability of a flat membrane, but also that the system could always reduce its grand potential energy by splitting a vesicle into two or more pieces, because each one would contribute with a constant amount $8\pi\kappa_s$ to Ω, independently of their radius. Of course, there should be a minimum radius for a vesicle, when R becomes less that 2 or 3 times the width of a membrane the system would be a lump of amphiphile molecules, without any resemblance to a spherical surface. It is relatively easy to find spherical density distributions of this type as local minima to the free energy. They do not have two concentric molecular layers with opposite orientations, as in vesicles, instead all the molecules are oriented with the head pointing out of the centre, a few examples are shown in figure 7(*a*)–(*c*). It is clear that these molecular aggregates correspond to the spherical micelles of the amphiphile molecules. We found an interesting variety of these

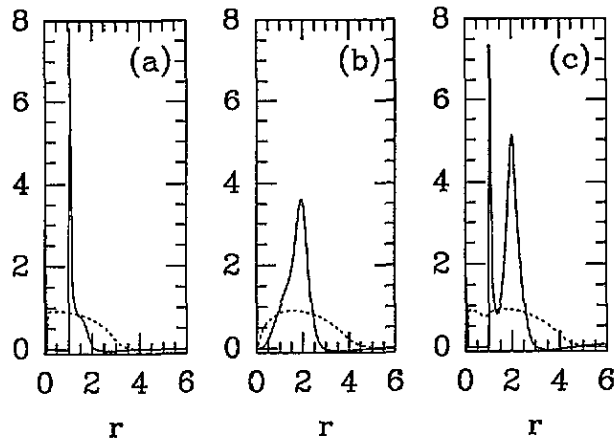

Figure 7. Radial density profiles and polar orientation order parameters for several types of micelles. The full lines are $(\rho(r) - \rho_0)r^2$, which give the representation of the density distribution better than $\rho(r)$. The dotted lines give $\eta(r)$, which is always positive, in contrast with vesicles and membranes. The three figures correspond to different interaction potentials and thermodynamic parameters: (a) uses Yukawa polar and quadrupolar interactions, with $\lambda = 3.$ and $q = 0.5$, bulk density $\rho_0 = 0.01$ and has excess of $\Delta N_m = 16.8$ molecules and $\Delta\Omega_m/(k_BT) = -1.57$, the peak at $r = 0$ contains a molecule surrounded by a spherical layer at $r \approx 1$ with a small shoulder. Figures (b) and (c) illustrate the difference between 'fluid' and 'solid' micelles, they correspond to the same temperature and interaction potential, which includes polar and quadrupolar interaction with a double Yukawa parametrization of $\Phi_2(r) = 0.5\Phi_1(r)$ and two different bulk densities: (b) represents a 'fluid' micelle for $\rho_0 = 0.01$ and (c) a 'solid' micelle for $\rho_0 = 0.012$.

micelles, depending on the thermodynamic parameters and on the details of the interaction potential, they have well defined density profile, excess of molecules ΔN_m, and excess of grand potential energy $\Delta\Omega_m$ over the homogeneous bulk. The smallest type of micelle we have found has a radial density profile $\rho(r)$ with a narrow peak in $r = 0$ which integrates to about one molecule, and a layer at a distance slightly larger that the hard-sphere diameter, which contains about 13 molecules. This is very close to the structure of a compact cluster of hard spheres, which reflects the good quality of our non-local description of the HS free energy in (3). Depending on the thermodynamic parameters, micelles may grow larger, either as a relatively unstructured lump (figure 7(*b*)) or with density strongly structured in concentric layers (figure 7(*c*)) but always with positive orientational order parameter η. We have observed micelles with up to a few hundred molecules but it is clear that their structure does not allow a continued growth. In the density functional space they are separated from vesicles by the inversion of the polar order in the internal molecular layer, and the depletion of the inner core. At particular temperatures we have observed two well differentiated types of micelles at the same thermodynamic conditions and, playing with the form of the interaction potential, we may even find 'micellar transitions', where the two different structures compete to be the most stable cluster. An interesting example is given by the coexistence of micelles with smooth and with sharp structure, like those illustrated in figures 7(*b*) and 7(*c*) respectively. With the simple Yukawa potential (11) the second class of structure is usually more stable than the first one, but with a smoother form for $\Phi_1(r)$, like a double Yukawa with opposite signs, we may change the balance and also make them coexist with the same value of $\Delta\Omega_m$. The most obvious interpretation of this fact is that we have 'fluid' and 'solid' micelles. The characterization of the latter is poor because our

variational parametrization of the density forces perfect radial symmetry, but we know that the density functional used for the HS free energy is quite accurate in the description of crystalline solids, if it is minimized within the appropriate family of density distributions. Of course, the excluded volume effects for real amphiphilic molecules are quite different from those of the hard spheres in our model and we should not take the detailed form of the micelles as a description of real amphiphilic aggregates. A more realistic description may be obtained using anisotropic hard-core interactions, but it would take our model out of our original aim of setting up a minimal model with different types of aggregation structures.

The micelles have an excess grand potential energy $\Delta\Omega_m$, over the homogeneous bulk, which depend on T and ρ_0. At the equilibrium line $\Delta\Omega_m$ is always well below the curvature energy $8\pi\kappa_s$ which gives the limit of (14) for vesicles of very small size, as may be expected since very small vesicles should reduce their grand potential by getting rid of the inner layer and becoming micelles, this trend is clear in figure 6, with the grand potential excess of small vesicles falling away from the straight line $A\sigma + 8\pi\kappa_s$. The total concentration of micelles in the solution may be calculated if we treat them as independent particles with internal grand potential energy $\Delta\Omega_m$ in chemical equilibrium with the solution of isolated molecules, although there is some uncertainty in the prefactor (as discussed in the next section), this density is proportional to $\exp(-\Delta\Omega_m/k_BT)$, so that in the (T, ρ_0) phase diagram (figure 4) we may draw a 'micellation line', $\rho_0^{mi}(T)$, where $\Delta\Omega_m$ changes sign. If the system presents more than one type of membrane, the relevant micellation line is given by the most stable aggregate. For $\rho_0 < \rho_0^{mi}(T)$, the micelles have positive excess of grand potential energy and they are scarce, for $\rho_0 > \rho_0^{mi}(T)$ they have negative excess of grand potential energy and they are abundant. Although there is not a sharp change, the exponential dependence of the micelle density on $\Delta\Omega_m$ reduces the interesting region to a narrow band around $\rho_0^{mi}(T)$, away from it we have no micelles at all, or there are so many that they interact with each other and form a dense phase of amphiphilic molecules. With our initial model interaction we found that $\rho_0^{mi}(T)$ was always well below the coexistence density for planar membranes, as is consistent with the negative values of the curvature energy. The conclusion was that the system would contain free molecules, micelles or dense phases, but not stable free membranes, despite the apparently correct phase diagram presented in the previous section. The negative curvature energies and the relative position of the micellation and the planar membrane equilibrium lines, show that the choice of the molecular interactions in our model is far from being irrelevant. Some choices of the potential energy $\Phi(\boldsymbol{r}, \hat{\boldsymbol{u}}_1, \hat{\boldsymbol{u}}_2)$ may give a phase diagram for planar membranes which is qualitatively correct, but they give values of κ_s and $\Delta\Omega_m$ which make the membranes unstable. This is the behaviour observed in many real amphiphilic solutions, where the micellar solution condensates directly in lamellar or hexagonal phases [4]. However, in some systems of strong amphiphiles the free membranes and vesicles coexist with the solution. In our model we searched for them with variations in the interaction potential. Changes in the form of the polar potential (11) were enough to produce positive curvature constants, without major changes in the phase diagram of planar membranes, but we always had $\rho_0^{mi}(T) < \rho_0^{eq}(T)$.

The global stabilization of the membranes was achieved with the inclusion of higher-order terms in the series expansion of the interaction potential (1). We included the twin terms with indices $(l_1 = 2, l_2 = 0, m = 0)$ and $(l_1 = 0, l_2 = 2, m = 0)$,

$$\Phi(\boldsymbol{r}_1 - \boldsymbol{r}_2, \hat{\boldsymbol{u}}_1, \hat{\boldsymbol{u}}_2) = \Phi_{HS}(r_{12}) + \sum_{i=1,2} \Phi_i(r_{12}) \left[P_i(\hat{\boldsymbol{u}}_1 \cdot \hat{\boldsymbol{r}}_{21}) + P_i(-\hat{\boldsymbol{u}}_2 \cdot \hat{\boldsymbol{r}}_{21}) \right] \tag{15}$$

where $P_i(x)$ are the Legendre polynomials and the function $\Phi_2(r) \equiv \xi_{20}^0(r) = \xi_{02}^0(r)$ represents the interaction of the quadrupolar order in one molecule with the isotropic average

of the other molecule. This term may be used to include the effect of anisotropic molecular cores, with stronger repulsion when a prolate molecule approaches another along its axis than when it approaches in a direction perpendicular to the molecular axis, which is a relevant factor for the curvature energy [5]. The minimization with respect to the molecular orientations is still done analytically, with two auxiliary fields now: the vector $a(r)$ defined in (8) and a tensor $\mathcal{B}(r)$ with components $b_{\alpha,\beta}$

$$b_{\alpha,\beta}(r_1) = \frac{1}{k_B T} \int \mathrm{d}r_2 \; \rho(r_2)\Phi_2(|r_1 - r_2|) \left[\frac{3\hat{r}_{21}^{\alpha}\hat{r}_{21}^{\beta} - \delta_{\alpha,\beta}}{2} \right] \tag{16}$$

where the indices α, β run over the three cartesian coordinates and $\hat{r}_{21}^{\alpha}$ are the components of the unit vector $\hat{r}_{21} = (r_2 - r_1)/r_{12}$. The tensor $\mathcal{B}$ is conjugated to the nematic order parameter [28]; it is symmetric and has zero trace. Both for planar and spherical geometries, the direction of the vector a and the main symmetry axis of $\mathcal{B}$ are given directly by the symmetry of the density distribution, and the problem is reduced to calculate the modulus $a(r) = |a(r)|$ and the largest eigenvalue of $\mathcal{B}$, which we call $b(r)$. The free energy density functional, already minimized with respect to the molecular orientations becomes:

$$\begin{aligned} F[\rho(r)] &= \mathrm{Min}\{F[\rho(r,\hat{u})]\}_{\alpha} \\ &= F_{HS}[\rho(r)] - k_B T \int \mathrm{d}r \rho(r) \log\left(Q(a(r), b(r))\right) \end{aligned} \tag{17}$$

with the function

$$Q(a,b) = \frac{1}{2}\int_{-1}^{1} \mathrm{d}x \exp(aP_1(x) + bP_2(x)) \tag{18}$$

which may be calculated in terms of the error function or the Dawson integral. There is no physical reason not to include in (15) other terms, like the 'polar–polar' interactions, $\xi_{11}^{-1}(r)$, $\xi_{11}^{0}(r)$ and $\xi_{11}^{1}(r)$, but any term coupling the molecular orientations of the two interacting molecules would make impossible the analytic minimization of the free energy with respect to the distribution of molecular orientations; we have chosen to keep this simplification. Moreover, we have taken $\Phi_2(r)$ proportional to $\Phi_1(r)$, with a proportionality factor q, which may be used to tune the properties of the system; the results described above correspond to $q = 0$.

In figure 4 we show the lines for the coexistence of planar membranes ($\sigma = 0$) (full lines) and for the micellation line ($\Delta\Omega_m = 0$) (dotted lines) for several values of q and λ. The two lines are nearly parallel in the plane $(\log \rho_0, T^{-1})$, which produces a strong sensitivity of the intersection with the parameters of the interaction potential. For example, for $\lambda = 2$ the lines cross each other at $\rho_0 = 0.018$ for $q = 0.5$ (curves B) but the intersection moves below $\rho_0 = 10^{-7}$ for $q = 0.3$ (curves A) and it has gone out of any reasonable range for the simple case $q = 0$ discussed above. Keeping q constant, the intersection also depends strongly on the range of the Yukawa potential. For $\lambda = 1.5$ and $q = 0.5$ (curves C) the intersection is at $\rho_0 = 0.0016$ and the two lines are much closer to each other than for $\lambda = 2$ and the same value $q = 0.5$ (curves B). In any case, the free membranes described in the previous section are truly stable along the line $\rho_0^{eq}(T)$ for values of ρ_0 below the intersection with $\rho_0^{mi}(T)$. The curvature energy is always positive, and it increases as ρ_0 and T decrease, as shown in figures 6 and 8 for $\lambda = 2$ and $q = 0.5$. Molecular interactions with a lower value of q give lower curvature energies. The persistence length for the local orientation of the membrane is estimated with effective surface hamiltonians [4] to go like $\exp(4\pi\kappa/3k_B T)$ in molecular units. Along the coexistence line this persistence length goes from 10^{29} at $\rho_0 = 10^{-6}$ to about 10^{6} at the intersection with the micellation line, all in units of the

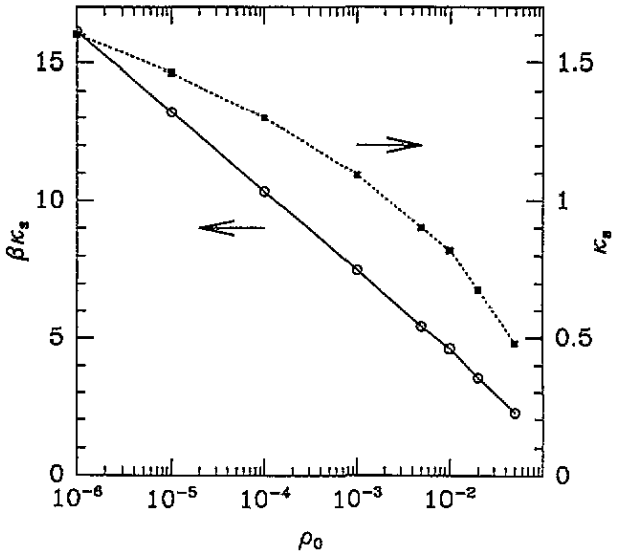

Figure 8. Spherical curvature energy, $\kappa_s = \kappa + \kappa_g/2$ along the coexistence line for membranes with polar and quadrupolar interactions (15) with the Yukawa potential with $\lambda = 2$ and $q = 0.5$. The full line gives $\beta\kappa_s = \kappa_s/(k_BT)$ and the dotted line gives κ_s/C, in units of the interaction strength. The horizontal axis gives the bulk density, in units of the HS diameter, but it also implies changes in the temperature to keep on the equilibrium line for membranes, as shown in figure 4(*b*).

HS diameter. Therefore, membranes of mesoscopic and even macroscopic sizes are well described by their representation as planar or spherical objects, with very little corrugation. As $\rho_0^{eq}(T)$ approaches the intersection with $\rho_0^{mi}(T)$ the membranes will coexist with an increasing number of micelles, as well as with the rarefied isolated amphiphilic molecules with density ρ_0. In the next section we present the global phase diagram which arises from this coexistence of different aggregates.

We have obtained results similar to those presented here for other forms of the interaction potential. Within the restrictions which we have already mentioned, they show the same qualitative features. The line of equilibrium for free membranes and the micellation line are never far from each other, and there are not always stable free membranes. The structure of the most stable micelles is more sensitive to changes in the interaction potential. The presence of a narrow maximum in $\Phi_1(r)$, for $r \approx 1$, favours the 'solid' micelles, with strong internal structure, while the 'fluid' micelles may be stabilized by interaction potentials with a smoother shape, which may be obtained with double Yukawa parametrizations.

5. Global phase diagram for membranes and micelles

In the preceding sections we have described a density functional model for a system of amphiphilic molecules, for which Ω has a large variety of local minima. Besides the trivial homogeneous density, which represents a dilute solution of independent molecules, we have characterized three types of molecular aggregates: planar membranes, spherical vesicles, and micelles of different types. Planar membranes and vesicles may be treated as 'macroscopic' phases in two dimensions, with extensive properties proportional to their area, and they coexist with the dilute bath when their surface tension σ vanishes. As

in the case of ordinary phase coexistence, the thermodynamic state of the system in the grand-canonical ensemble becomes degenerate: planar membranes and spherical vesicles of any size may appear if a reservoir provides the molecules to build them. The canonical ensemble gives a more realistic picture, with the membranes or vesicles growing from the molecules in the solution, until the bulk density is depleted to the equilibrium value $\rho_0^{eq}(T)$. The total area of the membranes is then fixed and the equilibrium shape will be determined by the 'marginal' contributions: the edge excess of grand potential energy and the curvature energy, $8\pi\kappa_s$, of closed vesicles. If the total amount of amphiphile in the system is only enough to build up a small membrane, the equilibrium shape would be a planar disk to minimize the edge line. If there were more molecules, the membrane would close itself into a vesicle, 'paying' the fixed curvature energy to avoid the edge [9]. As we said in the introduction we are pinning the molecular aggregate to a particular position and orientation, and we restrict its shape to planar or spherical symmetries. In this way we are neglecting the entropy associated to the fluctuation of the shape which, in the long-wavelength limit, would delocalize the membrane. This effects may be included within an effective surface hamiltonian, as capillary waves may be added to the 'intrinsic' liquid–vapour interface described by a density functional approximation, but there is always the uncertainty about the cut-off for the fluctuations included at the microscopic level. Nevertheless, as in the case of liquid–vapour interfaces, there is a reasonable window in the size of the membrane in which we may neglect these effects without major changes in the coexistence phase diagram.

The case of micelles is qualitatively different. They have well defined sizes, excess of molecules ΔN_m and excess of grand potential energy $\Delta\Omega_m$. A single micelle cannot be considered a macroscopic phase, because it has no extensive properties, they have to be considered as 'microscopic' molecular clusters. The 'true' structure of the homogeneous solution of amphiphilic molecules in water would contain these micelles, as well as isolated amphiphilic molecules and any other possible cluster structure. If we had a much better approximation for the density functional free energy, which were able to include the effects of simultaneous correlations between ΔN_m molecules, the homogeneous bulk phase would contain the micelles directly. However, our ignorance of such density functional free energy forces us to look for approximations linking the two levels of description. Our simple density functional does not include the correlations between many molecules, but it gives a good description for inhomogeneous systems and any correlation structure may be transformed in an inhomogeneous density distribution by an external pinning potential. The existence of a relative minimum of the grand potential energy for a non-uniform density distribution with low values of $\Delta\Omega_m$ is a signature that this particular structure may be produced by a very small pinning potential and it should be a very frequent correlation structure. However, the approximate density functional description of the micelle does not give a clear separation between the internal degrees of freedom and those associated to the collective movement which should be added.

Here we are considering only the case of dilute solutions, which allows us to neglect the interaction between micelles and to treat them as the components of an ideal gas. The configurational entropy per unit volume of the system with a density of micelles, ρ_m is given by:

$$S_m/V = -k_B\rho_m[\log(\rho_m\, v_m) - 1] \tag{19}$$

where v_m is the 'configurational unit cell' volume used to transform the volume in the classical phase space into a dimensionless number of states. All the uncertainty associated with the mixing of the two description levels is contained in this parameter. The equivalent

unit cell volume for a single amphiphilic molecule v_0, should appear in the ideal gas free energy (4), but we know that within classical statistical mechanics the value of v_0 is irrelevant for any measurable property, we may always get rid of it as a trivial shift of the origin for the chemical potential. This was done in (4), taking a dimensionless density in units of the HS diameter, d_{HS}, and transferring the irrelevant constant $k_BT \log(v_0 d_{HS}^{-3})$ into the chemical potential μ. We may interpret the free energy excess ΔF_m, in the density functional description of micelles, as the internal free energy of the aggregates and (19) as their translational entropy. Then it is straightforward to get the density of micelles at chemical equilibrium with the bath of amphiphilic molecules. As we may assemble a new micelle from ΔN_m free molecules, the chemical potential of a whole micelle is ΔN_m times $\mu_0 = \mu_{HS}(\rho_0)$, which gives

$$\rho_m = \frac{1}{v_m} \exp\left(-\frac{\Delta\Omega_m}{k_BT}\right) \tag{20}$$

where v_m gives the inverse volume dimension of the density ρ_m. The exponential dependence on $\Delta\Omega_m$ dominates the variation of ρ_m and this fact was used in the previous section to identify the 'micellation line', given by $\Delta\Omega_m = 0$, as the location of the narrow band, in the (T, ρ_0) plane, since the beginning of the formation of micelles to the saturation of the system with so many micelles that they start interacting with each other.

Nevertheless, the global phase diagram of the system should give the total concentration of amphiphilic molecules in the solution, ρ_t, when the membranes are in equilibrium. From the line $\rho_0^{eq}(T)$ obtained in section 2, we obtain a line $\rho_t^{eq}(T)$, through the relation:

$$\rho_t(\rho_0, T) = \rho_0 + \rho_m(\rho_0, T)\ \Delta N_m(\rho_0, T) \tag{21}$$

which requires the specification of v_m in (20). As we said in the introduction, the problem has been addressed in different ways in the literature. If we interpret that the density functional approximation gives a 'centre of mass' description of the micelle, we are tempted to get the entropy (19) as that of a free particle with the total excess of mass of the micelle, $\Delta N_m\ m$, where m is the molecular mass of the amphiphile [6]. Then v_m is associated to the 'thermal wavelength' of a molecule and a micelle, i.e.

$$v_m = \Lambda_m^3 = \frac{\hbar^3}{[2\pi k_BT \Delta N_m m]^{3/2}}. \tag{22}$$

However, we are working in classical statistical mechanics, and all the equilibrium properties associated to the position and spatial correlation of molecules should be independent of the molecular mass, which goes away in the momentum integrals, and is of course independent of the value of $\hbar$. It is hard to believe that the density of micelles in a solution of amphiphilic molecules in water, at room temperature, is controlled by quantum effects, so it is unlikely that equation (22) is the answer to our problem. Intuition may suggest that v_m has to be related to the 'natural' length units given by the intermolecular potential, i.e. the 'size' of the molecules, so in units of the HS diameter v_m should be proportional to ΔN_m^{α}, with a not too large value of $|\alpha|$. This intuition may be combined with (22) to indicate retention of only the dependence on the number of molecules, $v_m = \Delta N_m^{-3/2}$ in the 'natural' units of volume [21].

In the context of droplet nucleation and the use of 'coarse grained' density functionals, one may integrate over the 'Goldstone mode' associated with the position of the droplet [22], which leads to a volume v_m

$$v_m \sim \left[\frac{1}{3}\int d\mathbf{r}\,(\nabla\rho(\mathbf{r}))^2\right]^{-3/2} \tag{23}$$

The proportionality factor is unknown, because it would depend on the 'coarse graining' length which may be associated with our approximate density functional, which again we may hope is not very different from the molecular size. For a droplet with a nearly homogeneous density everywhere except in the surface, equation (23) gives $v_m \sim \Delta N_m^{-1}$, very different from (22), although for a vesicle they would agree. In the case of micelles, the value of v_m given by equation (23) depends strongly on the internal structure of the micelle. Thus for a 'solid' micelle, with strong structure of concentric layers, the result of (23) may be many orders of magnitude smaller than for a 'fluid' micelle of the same size. Thus, equation (23) would give a density of 'solid' micelles which is many orders of magnitude larger than that of coexisting 'fluid' micelles, with the same value of $\Delta\Omega_m$. This unphysical result reflects the lack of connection between the approximate description of the free energy in (3) and a coarse graining scale.

In the appendix we present a simple model which clarifies the problem. It is a simple harmonic molecule at chemical equilibrium with an ideal rarefied gas of their constituents atoms. The model may be solved exactly, to get the density of molecules as a function of the density of the atoms. Then we study the problem with a mean field approximation, which describes the molecule as an inhomogeneous density distribution, with an excess grand potential energy $\Delta\Omega_m$. The exact solution has a free translational mode and $n-1$ vibrational modes contributing to the free energy, while in the approximate mean field calculation there is no free translational mode (which requires the correlated movement of all the atoms) and all the n modes have positive frequencies. The ghost of the lost free translation mode appears as an indeterminacy in the position of the density distribution which describes the molecule. Now we may use equation (17) with the exact value of ρ_m and the approximate $\Delta\Omega_m$ to get v_m. As we anticipated it has no dependence with the particle mass or with the 'thermal wavelength'. It gets its dimension from the ratio between the spring constant of the harmonic forces and the thermal energy k_BT. A natural extension to our problem is through the connection of the spring constant with the 'molecular compressibility', i.e. to the change in the molecular size induced by external pressure. Thus, we propose here to take

$$v_m = \left[\frac{k_BT}{\Delta N_m}\int \mathrm{d}r\ \frac{\mathrm{d}}{\mathrm{d}p_0}\left[\log(\rho(r)/\rho_0)\right]\right]^{1/2} \tag{24}$$

where $p_0 = p_{HS}(\rho_0)$ is the pressure of the bulk phase. This approximation for v_m goes together with the approximate free energy used to evaluate $\Delta\Omega_m$. Any description of the molecular aggregates as self-structured density distributions is an approximation. If we could use the exact free energy density functional of the problem we would get the presence of micelles from the correlation structure, but the equilibrium density distribution in the absence of external potentials will be homogeneous. There is no exact value of v_m in (20) because there is no exact value of $\Delta\Omega_m$, and we should take together the approximation in the two terms. Our proposal is reasonable, it may be used for any density functional approximation, without any other ingredient like the molecular mass or the 'coarse graining' length, and it gives, in a natural way, values of v_m which are related to the molecular size.

We may now calculate the global phase diagram, in figure 9, with the total density of amphiphilic molecules at equilibrium with free membranes calculated with (20), (21) and (24). The phase diagram shows a low-temperature region in which free membranes coexist with the amphiphilic solution nearly in absence of micelles ($\rho_t \simeq \rho_0^{eq}(T)$). As this coexistence line approaches the region of micellation there is a sharp bend in the curve. We have to add a much larger amount of amphiphile to keep the free membranes stable, most of it goes into micelles, with very little increase of ρ_0. This fact sets a maximum

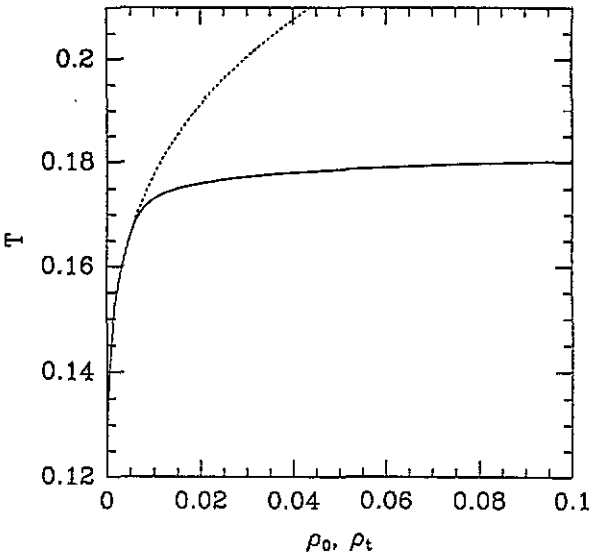

Figure 9. Global phase diagram for free membranes with polar and quadrupolar interactions (15) with the Yukawa potential with $\lambda = 2$ and $q = 0.5$. The dotted line represent the equilibrium line $\rho_0^{eq}(T)$, as in figure 4(*b*), in terms of the density of isolated amphiphilic molecules, ρ_0, while the full line represents the total density of amphiphilic molecules, including isolated molecules and micelles, at equilibrium with free membranes at each temperature, in units of the interaction strength. We represent only the low-density part of the diagram, with $\rho_t < 0.1$ in units of the HS diameter, where the micelles may be treated as isolated aggregates.

temperature for the existence of free membranes which is close to the crossing of $\rho_0^{eq}(T)$ and the micellation line, where the system becomes packed with micelles and we have to go beyond the ideal gas approximation for them. The difference between the two lines in the phase diagram in figure 9 shows the importance of the global analysis to predict the stability of membranes in the relevant thermodynamic space (ρ_t, T), rather than in (ρ_0, T).

We conclude that the density functional model developed here contains the essential feature of amphiphilic systems: a large variety of aggregation structures from microscopic clusters to macroscopic phases. We have explored only molecular distributions with perfect planar and spherical geometry. The same density functional may be used to study other cases, with computational capability the only limitation. It is clearly feasible to study aggregates with cylindrical symmetry, which would allow the calculation of the two independent curvature energy constants and also to study the stability of rod-like micelles and hexagonal phases, induced by a intrinsic preferential curvature produced by other terms in the molecular potential. It is also possible, with the present computational power, to study systems in which the density distribution depends on two variables, like a semi-infinite planar membrane to calculate the edge energy, when it is free or anchored to a substrate. All these properties would refer to the same density functional approximation. They would be consistently linked at microscopic level, and this link may pose more restrictions on the detailed interactions in our model. In our attempt to set up a minimal model, we have eliminated many aspects of the molecular structure and interactions, e.g. the flexible hydrocarbon tails and the detailed interaction with water, which are crucial to determine the structure of the aggregates in real amphiphiles. The molecular structure of micelles in our model is very different from that of real amphiphilic micelles. However, as in any complex system, we may hope that the most relevant features are common to a broad class

of systems, and the main role of the theoretical models is precisely to find out simple realizations of the class. In this case, the existence of a large variety of aggregates with very different geometries is the main feature shared by our model and amphiphilic systems. The approximations in the density functional, and in the connection of the two levels of descriptions for micelles, may be checked directly in computer simulations, either with the full molecular description, or with the exact analytic average over the molecular orientations. The validation of the approximation for this minimal model would be of interest for the development of more complex descriptions of the amphiphilic molecules.

Acknowledgments

We are grateful to D E Sullivan and M M Telo da Gama for useful comments, at different stages in the realization of this work, and to J P Hernandez for careful reading of the manuscript. This work was supported by the Dirección General de Investigación Científica y Técnica of Spain, under grant number PB91-0090.

Appendix

Here we present a simple model for which we may calculate the prefactor v_m in (20), by comparing the result of a mean field approximation with the exact solution. We consider a linear harmonic molecule formed by n classical particles of equal mass, m, which move along the X axis linked with $n-1$ equal springs of constant κ. We denote by x_i and p_i the coordinate and momentum of each particle, with $i = 1, \ldots, n$, and the hamiltonian is

$$H_m(x_1, \ldots, x_n, p_1, \ldots, p_n) = \frac{1}{2m}\sum_{i}^{n} p_i^2 - U_0 + \frac{\kappa}{2}\sum_{i=1}^{n-1}(x_{i+1} - x_i - l_0)^2 \tag{A1}$$

where U_0 and l_0 are the molecular binding energy and equilibrium atomic distances. These molecules are at chemical equilibrium with an ideal gas of monomers, with kinetic energy $p^2/(2m)$. We use classical statistical mechanics to describe a mixture of N_0 indistinguishable monomers and N_m indistinguishable n-mers molecules, without any interaction. The total free energy in a one-dimensional box of length L is:

$$F(T, L, N_0, N_m) = k_B T\left(N_0\left[\log\left(\frac{N_0}{z_0}\right) - 1\right] + N_m\left[\log\left(\frac{N_m}{z_m}\right) - 1\right]\right) \tag{A2}$$

where z_0 and z_m are the partition function of a monomer and a molecule respectively. For the monomer in a box of length L we may write, $z_0 = L/v_0$, where v_0 is the 'configurational unit length' (or thermal wavelength) for monomers,

$$v_0 = \hbar\left[\frac{2\pi}{k_B T\, m}\right]^{1/2} \tag{A3}$$

and $\hbar$ is the quantum of phase space (within classical statistical mechanics it may be taken as an arbitrary constant without any change in observable properties). For the molecules we have to take into account the harmonic vibrations of the $n-1$ normal modes, with frequencies $\omega_i > 0$, and the free translation of the centre of mass. The latter contributes to z_m with a factor $n^{1/2}\, L/v_0$, each vibration mode contributes with a factor $k_B T/(\hbar\omega_i)$ and there is a factor $e^{U_0/k_B T}$ from the molecular binding energy.

The chemical potential of monomers and molecules, when they have density $\rho_0 = N_0/L$ and $\rho_m = N_m/L$ respectively, are directly obtained from (A2):

$$\mu_0 = \frac{\partial F}{\partial N_0} = k_B T \log(\rho_0 v_0) \qquad \mu_m = \frac{\partial F}{\partial N_m} = k_B T \log\left[\frac{\rho_n v_0}{n^{1/2}} \prod_{i=1}^{n-1} \left(\frac{\hbar\omega_i}{k_B T}\right)\right] - U_0. \quad \text{(A4)}$$

The equilibrium between monomers and molecules implies that $\mu_m = n\mu_0$, because we can make a molecule from n monomers and vice versa. This gives the exact equilibrium density of molecules as a function of ρ_0 and T,

$$\rho_m = \rho_0^n \, v_0^{n-1} e^{U_0/k_B T} n^{1/2} \prod_{i=1}^{n-1} \left(\frac{k_B T}{\hbar\omega_i}\right) \quad \text{(A5)}$$

with the usual form of the chemical equilibrium in ideal gases or solutions. We may define the dimensionless frequencies, $\hat{\omega}_i = \omega_i (m/\kappa)^{1/2}$, which are independent of both m and κ, and are the $n-1$ positive roots of the characteristic equation

$$\begin{vmatrix} 1-\hat{\omega}^2 & -1 & 0 & \dots & & & \\ -1 & 2-\hat{\omega}^2 & -1 & 0 & \dots & & \\ 0 & -1 & 2-\hat{\omega}^2 & -1 & 0 & \dots & \\ \dots & \dots & \dots & \dots & \dots & \dots & \dots \\ & \dots & 0 & -1 & 2-\hat{\omega}^2 & -1 & 0 \\ & & \dots & 0 & -1 & 2-\hat{\omega}^2 & -1 \\ & & & \dots & 0 & -1 & 1-\hat{\omega}^2 \end{vmatrix} = 0 \quad \text{(A6)}$$

while the remaining root is $\omega = 0$, associated to the free translation of the molecule. In this way we arrive at,

$$\rho_m = \rho_0^n e^{U_0/k_B T} n^{1/2} \prod_{i=1}^{n-1} \left(\frac{k_B T}{\kappa\hat{\omega}_i^2}\right)^{1/2} \quad \text{(A7)}$$

which is independent of both $\hbar$ and m, as it has to be in classical statistical mechanics. The only relevant length scale which appears to settle the dimension balance comes from the ratio between the thermal energy $k_B T$ and the spring constant κ.

Let us now analyse the problem along the lines used in this work to describe molecular aggregates. We use a mean field approximation, which corresponds to studying the vibrations of each particle in the molecule with all the other particles at their equilibrium positions x_i^{eq}. With this approximation we obtain a vibration mode for each particle in the molecule, all frequencies are proportional to $(\kappa/m)^{1/2}$ with proportionality factors $\hat{\omega}_i^{mf}$, which come from the diagonal terms of (A6). In this mean field treatment the density distribution of particles in a molecule is given by gaussian peaks centred around each equilibrium position x_i^{eq} and width proportional to $(k_B T/\kappa)^{1/2}$. The relative distance between the peaks is given by l_0 in (A1), but the overall position of the molecule is not determined. The total free energy of a molecule, in this mean field approximation is:

$$\Delta F_m = -U_0 - k_B T \sum_{i=1}^{n} \log\left[\frac{k_B T}{\hbar\omega_i^{mf}}\right] = -U_0 - k_B T \sum_{i=1}^{n} \log\left[\frac{(k_B T)^{1/2}}{\kappa^{1/2} v_0 \hat{\omega}_i^{mf}}\right]. \quad \text{(A8)}$$

Both ΔF_m and the chemical potential μ_0 depend on v_0 but this dependence cancels out in the grand potential excess,

$$\Delta\Omega_m = \Delta F_m - \mu_0 n = -U_0 - k_B T \sum_{i=1}^{n} \log\left[\frac{(k_B T)^{1/2}\rho_0}{\kappa^{1/2}\hat{\omega}_i^{mf}}\right]. \quad \text{(A9)}$$

We now use this approximate grand potential energy to get the density of molecules at equilibrium with the ideal gas of monomers, as a function of T and ρ_0. This is done through equation (20) and we may compare with the exact result (A7) to get the value of the undetermined parameter v_m, which represents the 'configurational unit cell' for the molecules:

$$v_m = \frac{e^{-\Delta\Omega_m/k_BT}}{\rho_m} = \left(\frac{k_BT}{\kappa}\right)^{1/2} n^{-1/2} \prod_{i=1}^{n-1} \hat{\omega}_i \Big/ \prod_{j=1}^{n} \hat{\omega}_j^{mf}. \tag{A10}$$

The first conclusion is that v_m gets its dimension of length from the factor $(k_BT/\kappa)^{1/2}$, which as we say above is the only natural length in the problem. This length is multiplied by a numerical factor which depends on the number of monomers n. For a dimer, $n = 2$, this factor is exactly 1, and it decays exponentially with n as $2^{(2-n)/2}$. This particular dependence is associated with the simple molecular structure defined in (A1), we may study other harmonic structures and find different numerical coefficients. Even for the model (A1) we may get other factors if we improve the approximation used to get $\Delta\Omega_m$. Thus, we could analyse the vibrations of each particle keeping the correlations with its first neighbours, but with the other particles fixed at their equilibrium positions. This would still give a representation of the molecule as a inhomogeneous density distribution, with wider gaussian amplitudes around each x_i^{eq}, and arbitrary origin. The normal frequencies from the approximate and the exact characteristic equations would approach, and the numerical factor in (A10) would become closer to 1. Only when we include the correlations between all the n particles in the molecule do we recover the soft mode of translation and lose the description of the molecule as a inhomogeneous density distribution.

For any approximate description of the molecule, we may express the exponential dependence with n in the numerical factor in (A10) as

$$\rho_m = \left(\frac{\kappa}{k_BT}\right)^{1/2} \exp\left[-\frac{\Delta\Omega_m}{k_BT} - \alpha(n-2)\right] \tag{A11}$$

where the exact value of ρ_m is taken from the approximate $\Delta\Omega_m$ by using the adequate value of α. The term $\alpha(n-2)$ may be understood as the correction of the error made by the approximate $\Delta\Omega_m$, and it has the correct linear dependence with the molecular size which may be expected in $\Delta\Omega_m$, which for large n should be an extensive quantity. The second conclusion is that, in the absence of the exact result, we may take

$$\rho_m = \left(\frac{\kappa}{k_BT}\right)^{1/2} \exp\left[-\frac{\Delta\Omega_m}{k_BT}\right] \tag{A12}$$

as the approximate density of aggregates, consistent with its description through the approximate $\Delta\Omega_m$. The uncertainty in a numerical prefactor is thrown into, and mixed with, the uncertainty in the degree of accuracy of the free energy approximation. This approximation leads to a v_m which is independent of the number of monomers in the molecule. The spring constant κ has an obvious interpretation in terms of the inverse 'molecular compressibility' χ_m, i.e. the change in the total molecular length, $\delta l_m = n\,\delta l_0$, induced by a external compression force δf,

$$\kappa^{-1} = n^{-1}\frac{\delta l_m}{\delta f} = \frac{l_m}{n}\chi_m \tag{A13}$$

which may be extended directly to molecular aggregates in three dimensions, with total excess of molecules ΔN_m, and the volume integral of the isothermal compressibility, $\chi_T = \partial(\log(\rho))/\partial p$, minus its bulk value, as the generalization of $l_m\chi_m$. This leads to the equation (24) used here to determine v_m.

References

[1] Lindman B 1985 *Physics of Amphiphiles: Micelles, Vesicles and Microemulsions* ed V Degiorgio and M Corti (Amsterdam: North-Holland)

[2] Seddon J M 1990 *Biochim. Biophys. Acta* **1031** 1

[3] Gelbart G W, Roux D and Ben-Shaul A (ed) 1994 *Micelles, Membranes and Monolayers* (Berlin: Springer)

[4] Gompper G and Schick M 1994 Self-assembling amphiphilic systems *Phase Transitions and Critical Phenomena* ed C Domb and J Lebowitz (London: Academic)

[5] Israelachvili J N 1985 *Physics of Amphiphiles: Micelles, Vesicles and Microemulsions* ed V Degiorgio and M Corti (Amsterdam: North-Holland)

[6] McMullen III W E, Gelbart M and Ben-Shaul A 1984 *J. Phys. Chem.* **88** 6649

[7] Helfrich W 1973 *Z. Naturf.* c **28** 693

[8] Nelson D, Piran T and Weinberg S (ed) 1989 *Statistical Mechanics of Membranes and Surfaces* (Singapore: World Scientific)

[9] Lipowski R 1991 *Nature* **349** 475

[10] Lipowski R, Richter D and Kremer K (ed) 1992 *The Structure and Conformation of Amphiphilic Membranes* (Berlin: Springer)

[11] Gennis R B 1989 *Biomembranes: Molecular Structure and Function* (Berlin: Springer)

[12] Gompper G and Schick M 1989 *Chem. Phys. Lett.* **163** 475

[13] Matsen M W and Sullivan D E 1990 *Phys. Rev.* A **41** 2021

[14] Halley J W and Kolan A J 1988 *J. Chem. Phys.* **88** 3313

[15] Gompper G and Klein S 1992 *J. Physique.* **2** 1725

[16] Evans R 1992 *Fundamentals of Inhomogeneous Fluids* ed D Henderson (New York: Marcel Dekker)

[17] Baus M 1990 *J. Phys.: Condens. Matter* **2** 2111

[18] Haymet A D J 1992 *Fundamentals of Inhomogeneous Fluids* ed D Henderson (New York: Marcel Dekker)

[19] Marko J F 1992 *Fundamentals of Inhomogeneous Fluids* ed D Henderson (New York: Marcel Dekker)

[20] Tarazona P 1993 *Phil. Trans. R. Soc.* A **344** 307

[21] Morse D C and Milner S T 1994 *Europhys. Lett.* **26** 565

[22] Gunton J D and Droz M 1983 *Introduction to the Theory of Metastable and Unstable States* (Berlin: Springer)

[23] de Gennes P G and Taupin C 1982 *J. Phys. Chem.* **86** 2294

[24] Gray C G and Gubbins K E 1984 *Theory of Molecular Fluids* vol I (London: Oxford University Press)

[25] Telo da Gama M M 1987 *Mol. Phys.* **62** 585
Telo da Gama M M and Gubbins K E 1986 *Mol. Phys.* **59** 227

[26] Tarazona P 1985 *Phys, Rev.* A **31** 2672
Tarazona P, Marini Bettolo Marconi U and Evans R 1987 *Mol. Phys.* **60** 573

[27] Helfrich W 1978 *Z. Naturf.* a **33** 305

[28] de Gennes P G 1974 *The Physics of Liquid Crystals* (London: Oxford University Press)